Available online at www.sciencedirect.com
SCIENCE DIRECT
Mathematics and Computers in Simulation 71 (2006) 404–414
MATHEMATICS AND COMPUTERS IN SIMULATION
www.elsevier.com/locate/matcom

Levitation–guidance stabilization of superconducting maglev through LSM currents

Tetsuzo Sakamoto *, Masaki Nakayama

Department of Control Engineering, Kyushu Institute of Technology, Tobata, Kitakyushu 804-8550, Japan

Available online 18 April 2006

Abstract

This paper presents a modeling and simulation of a superconducting maglev vehicle with a levitation and guidance assist method we have proposed. The assist system stabilizes and assists the vehicle operation so that the vehicle does not need to depend on the mechanical wheels as much as possible at low speeds. By controlling the LSM armature currents, the auxiliary levitation and guidance forces are provided. The results show that the assist system produces appropriate levitation and guidance forces, establishing the reference levitation height and a sufficient guidance at low speeds even against the disturbance force of lateral wind.

Keywords: LSM; Magnetic levitation; Guidance; Stabilization; Maglev

1. Introduction

Levitation and guidance forces of a superconducting maglev vehicle result from the passive electrodynamic phenomena between the onboard SCMs and the levitation–guidance coils installed on the ground. The vehicle is propelled by the armature coil currents of the linear synchronous motor (LSM) installed on the ground. Since the levitation force is relatively small and pulsative below some speed due to its nature, the vehicle motion stability is poor at low speeds and the minimum levitating speed is limited at around 100 km/h as well. We have so far proposed and discussed the methodologies for propulsion control and guidance control in terms of *dq*-axis electromagnetic variables of the superconducting linear synchronous motor (LSM) vehicle [2–4,6]. When we view the three-phase circuit variables of LSM on the *dq*-axis, the force between the *q*-axis LSM armature currents and the field from the onboard SCMs translates to the propulsion force. Then if the force is formulated appropriately to include all the space harmonic components, the thrust coefficient can be defined, making it possible to discuss the electrodynamic forces of the air-cored LSM vehicle rigorously [6,2], whereas conventional analyses had been treated in the same manner as a rotary motion machine. On the other hand, the *d*-axis component is associated with the normal and lateral forces of the LSM, the former of which can lead to the definition of the *normal force coefficient*; for the current model of interest we are tackling to, it is redefined as the *guidance force coefficient* because the plane of the LSM is perpendicular to the horizon [4]. The latter force can then be utilized for levitation in our model [5]. Thus, we aim to control the LSM armature currents to generate guidance and levitation forces of the vehicle as well as propulsion forces. This paper presents the modeling and simulation of the maglev vehicle stabilization system to produce assist levitation and guidance forces with the

* Corresponding author. Fax: +81 93 861 1159.
E-mail address: sakamoto@cntl.kyutech.ac.jp (T. Sakamoto).

0378-4754/$32.00
doi:10.1016/j.matcom.2006.02.024

levitation–guidance coils taken into account. The results show the system works well with the LSM armature current control at low speeds where mechanical suspension is needed.

2. Electrodynamic analysis

2.1. Levitation force of levitation–guidance coils

The schematic diagram for the analysis is shown in Fig. 1. Levitation forces are generated by the inductive interactions between the 8-figure levitation coils on the ground and the onboard SCMs, which increase monotonously with increasing the vehicle running speed. At very low speeds, the vehicle suspension depends on mechanical wheels because levitation and guidance forces are small and that the rolling stiffness stemming from the electrodynamic interaction is relatively small.

First we formulate the electrodynamic relationships on the levitation–guidance coils. The y-axis component flux density generated from the onboard SCMs is given in terms of vehicle coordinate system (x,y,z) as

$$B_{sy} = -\frac{\mu_0}{2} \sum_{k=1,3,\ldots}^{\infty} \sum_{m=1,3,\ldots}^{\infty} \beta_{km} a_s(k,m) \sin(\alpha_k x) \cos(\alpha_m z) e^{-\beta_{km}(y-d_s)} \tag{1}$$

where $\alpha_k = \pi k/L$, $\alpha_m = \pi m/W$, $\beta_{km} = \sqrt{\alpha_k^2 + \alpha_m^2}$:

$$a_s(k,m) = \frac{16 n_s I_s}{\pi^2 k m} \sin\left(\alpha_k \frac{l_s}{2}\right) \sin\left(\alpha_m \frac{w_s}{2}\right) \frac{\sin(4\alpha_k \tau)}{\cos(\alpha_k \tau/2)}$$

d_s is the distance of SCM from the vehicle center (see Fig. 1), τ the pole pitch, l_s, w_s the length and width of SCM and $n_s I_s$ is the mmf of SCM. Two coordinate systems are used for the analysis as shown in Fig. 1, where the relationship is defined as

$$(x' - x, y' - y, z' - z) = (x_1, y_1, z_1)$$

We then obtain the flux linkage of the levitation–guidance coil with an 8-figure shape located at $x' = 0$:

$$\psi_1 = -\sum_k \sum_m \Psi_{km} k_{lc} \sin(\alpha_k v_x t) e^{-\beta_{km}(d_l - d_s - y_1)} \sin \alpha_m \Delta z = \mathrm{Re} \sum_k \dot{\Psi}_{km} k_{lc} e^{j\omega_k t} \tag{2}$$

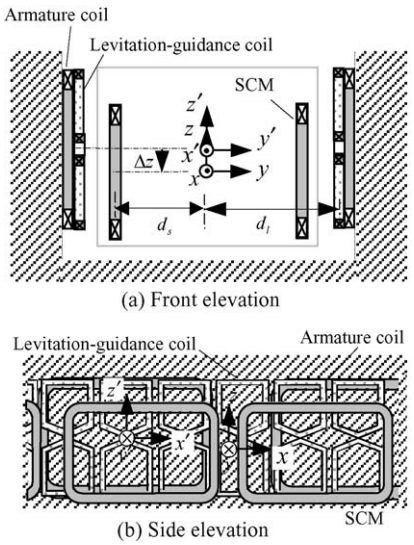

Fig. 1. Schematic diagram of the model.

where

$$\dot{\Psi}_{km} = \mathrm{j}\sum_{m} \Psi_{km}\, \mathrm{e}^{-\beta_{km}(d_\mathrm{l}-d_\mathrm{s}-y_1)} \sin\alpha_m \Delta z, \quad \omega_k = \alpha_k v_x$$

$$\Psi_{km} = n_\mathrm{l}\frac{\mu_0}{2}\beta_{km} a_\mathrm{s}(k,m) p_{lkm}, \quad z' - z = -\Delta z$$

$$p_{\mathrm{l}km} = \frac{8}{\alpha_k}\sin\alpha_k \frac{l_\mathrm{l}}{2}\sin\alpha_m \frac{w_\mathrm{l}}{2}, \quad k_\mathrm{lc} = \sin\alpha_m \frac{c_\mathrm{l}}{2}$$

l_l, w_l: length and width of levitation–guidance coil, c_l: distance between the upper and the lower loop of the levitation–guidance coil.

The voltage equation is given by using the electrical resistance R_l and the self-inductance L_l of the levitation coil as follows [5]:

$$R_\mathrm{l} i_\mathrm{l} + L_\mathrm{l}\frac{\mathrm{d}i_\mathrm{l}}{\mathrm{d}t} = -\frac{\mathrm{d}\psi_\mathrm{l}}{\mathrm{d}t} \tag{3}$$

We obtain the solution in the phasor form of the differential equation as

$$i_\mathrm{l} = \mathrm{Re}\sum_{k} \dot{I}_{lk}\, \mathrm{e}^{\mathrm{j}\omega_k t} \tag{4}$$

$$\dot{I}_{\mathrm{l}k} = \frac{\omega_k}{R_\mathrm{l} + \mathrm{j}\omega_k L_\mathrm{l}} \sum_{m} \Psi_{km} k_\mathrm{lc}\, \mathrm{e}^{-\beta_{km}(d_\mathrm{l}-d_\mathrm{s}-y_1)} \sin(\alpha_m \Delta z) \tag{5}$$

where $z_2(t) = 0$ was assumed.

If we take all the associated levitation coils with the corresponding vehicle levitation force into account, then we obtain the time average value of the vehicle levitation force as

$$F_{L_\mathrm{l}} = -\frac{L}{\tau_\mathrm{l}}\sum_{k} \mathrm{Re}\left(\dot{I}_{\mathrm{l}k}\frac{\partial \dot{\Psi}^*_{\mathrm{l}k}}{\partial z_1}\right)\Bigg|_{z_1=\Delta z} = \frac{L}{\tau_\mathrm{l}}\sum_{k} \frac{\omega_k^2 L_\mathrm{l}}{R_\mathrm{l}^2 + \omega_k^2 L_\mathrm{l}^2} \left\{\sum_{m} \Psi_{km} k_\mathrm{lc}\, \mathrm{e}^{-\beta_{km}(d_\mathrm{l}-d_\mathrm{s}-y_1)} \sin(\alpha_m \Delta z)\right\}$$
$$\times \left\{\sum_{m} \alpha_m \Psi_{km} k_\mathrm{lc}\, \mathrm{e}^{-\beta_{km}(d_\mathrm{l}-d_\mathrm{s}-y_1)} \cos(\alpha_m \Delta z)\right\} \tag{6}$$

2.2. Guidance force of levitation–guidance coils

Fig. 2(a) shows the connection of the guidance–levitation coils, where the null-flux cable works when the vehicle does not run at the center, causing vehicle guidance forces. Fig. 2(b) describes the equivalent circuits for guidance, while the unfolded circuits are shown in Fig. 2(c). The resultant flux linkage of the upper levitation–guidance coils is given by the equation:

$$\psi_\mathrm{Gu} = \psi_\mathrm{Gur} - \psi_\mathrm{Gul} = \mathrm{Re}\sum_{k=1,3,\cdots}^{\infty} \dot{\Psi}_{\mathrm{Gu}k} \exp(\mathrm{j}\omega_k t) \tag{7}$$

where

$$\dot{\Psi}_{\mathrm{Gu}k} = \mathrm{j}\sum_{m} \left[\Psi_{km} \exp\{-\beta_{km}(d_\mathrm{l} - d_\mathrm{s})\} \cos\left\{\alpha_m\left(\Delta z + \frac{c_\mathrm{l}}{2}\right)\right\} \sinh(\beta_{km} y_1)\right.$$

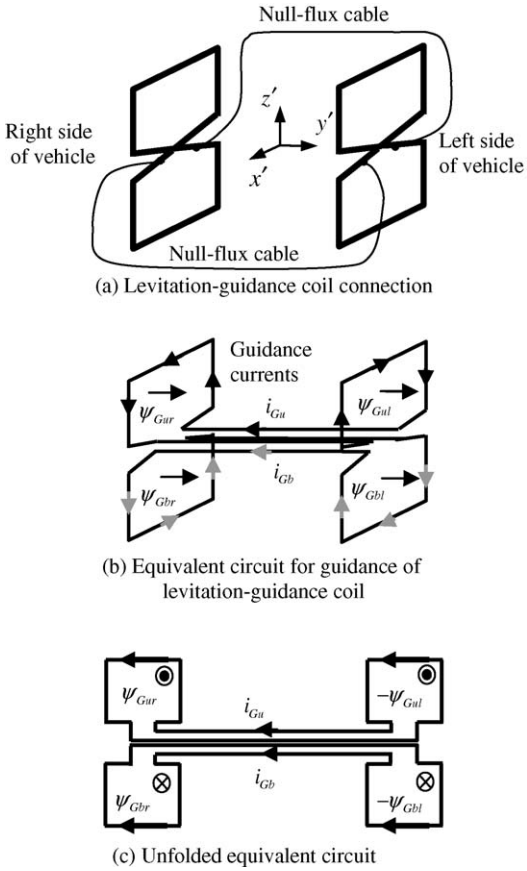

Fig. 2. Levitation–guidance coil currents.

The resultant flux linkage of the lower levitation–guidance coils is expressed as

$$\psi_{\mathrm{Gb}} = \psi_{\mathrm{Gbr}} - \psi_{\mathrm{Gbl}} = \mathrm{Re} \sum_{k=1,3,\cdots}^{\infty} \dot{\Psi}_{\mathrm{Gb}k} \exp(j\omega_k t) \tag{8}$$

where

$$\dot{\Psi}_{\mathrm{Gb}k} = j\sum_{m} \left[\Psi_{km} \exp\{-\beta_{km}(d_{\mathrm{l}} - d_{\mathrm{s}})\} \cos\left\{ \alpha_m \left(\Delta z - \frac{c_{\mathrm{l}}}{2} \right) \right\} \sinh(\beta_{km} y_{\mathrm{l}}) \right.$$

Substituting (7) and (8) into the circuit equations for both upper and lower coils:

$$R_{\mathrm{G}} i_{\mathrm{Gu}} + L_{\mathrm{G}} \frac{\mathrm{d}i_{\mathrm{Gu}}}{\mathrm{d}t} + M_{\mathrm{G}} \frac{\mathrm{d}i_{\mathrm{Gb}}}{\mathrm{d}t} = -\frac{\mathrm{d}\psi_{\mathrm{Gu}}}{\mathrm{d}t} \tag{9}$$

$$R_{\mathrm{G}} i_{\mathrm{Gb}} + L_{\mathrm{G}} \frac{\mathrm{d}i_{\mathrm{Gb}}}{\mathrm{d}t} + M_{\mathrm{G}} \frac{\mathrm{d}i_{\mathrm{Gu}}}{\mathrm{d}t} = -\frac{\mathrm{d}\psi_{\mathrm{Gb}}}{\mathrm{d}t} \tag{10}$$

we get the following approximated solutions of currents:

$$i_{\mathrm{Gu}} = \mathrm{Re} \sum \dot{I}_{\mathrm{Gu}k} \exp(\mathrm{j}\omega_k t) \tag{11}$$

$$i_{\mathrm{Gb}} = \mathrm{Re} \sum \dot{I}_{\mathrm{Gb}k} \exp(\mathrm{j}\omega_k t) \tag{12}$$

where

$$\dot{I}_{\mathrm{Gu}k} \cong \frac{\omega_k}{R_\mathrm{G} + \mathrm{j}\omega_k L_\mathrm{G}} \sum_m \left[\Psi_{km} \exp\{-\beta_{km}(d_\mathrm{l} - d_\mathrm{s})\} \cos\left\{ \alpha_m \left(\Delta z + \frac{c_\mathrm{l}}{2} \right) \right\} \sinh(\beta_{km} y_1) \right]$$

$$\dot{I}_{\mathrm{Gb}k} \cong \frac{\omega_k}{R_\mathrm{G} + \mathrm{j}\omega_k L_\mathrm{G}} \sum_m \left[\Psi_{km} \exp\{-\beta_{km}(d_\mathrm{l} - d_\mathrm{s})\} \cos\left\{ \alpha_m \left(\Delta z - \frac{c_\mathrm{l}}{2} \right) \right\} \sinh(\beta_{km} y_1) \right]$$

R_G, L_G: electrical resistance and self-inductance of the levitation–guidance coil for guidance action.

We then obtain the guidance forces as

$$\begin{aligned} F_\mathrm{Gg} &= -\frac{1}{2}\frac{L}{\tau_\mathrm{l}} \sum_k \mathrm{Re}\left(\dot{I}_{\mathrm{Gu}k} \frac{\partial \dot{\Psi}^*_{\mathrm{Gu}k}}{\partial y_1} + \dot{I}_{\mathrm{Gb}k} \frac{\partial \dot{\Psi}^*_{\mathrm{Gb}k}}{\partial y_1} \right) \\ &= \frac{1}{2}\frac{L}{\tau_\mathrm{l}} \sum_k \left[\frac{\omega_k^2 L_\mathrm{G}}{R_\mathrm{G}^2 + \omega_k^2 L_\mathrm{G}^2} \left\{ \sum_m \Psi_{km} \exp(-\beta_{km}(d_\mathrm{l} - d_\mathrm{s})) \cos\left(\alpha_m \left(\Delta z + \frac{c_\mathrm{l}}{2} \right) \right) \sinh(\beta_{km} \Delta y) \right\} \right. \\ &\quad \left. \times \left\{ \sum_m \Psi_{km} \beta_{km} \exp(-\beta_{km}(d_\mathrm{l} - d_\mathrm{s})) \cos\left(\alpha_m \left(\Delta z + \frac{c_\mathrm{l}}{2} \right) \right) \cosh(\beta_{km} \Delta y) \right\} \right] \\ &\quad + \frac{1}{2}\frac{L}{\tau_\mathrm{l}} \sum_k \left[\frac{\omega_k^2 L_\mathrm{G}}{R_\mathrm{G}^2 + \omega_k^2 L_\mathrm{G}^2} \left\{ \sum_m \Psi_{km} \exp(-\beta_{km}(d_\mathrm{l} - d_\mathrm{s})) \cos\left(\alpha_m \left(\Delta z - \frac{c_\mathrm{l}}{2} \right) \right) \sinh(\beta_{km} \Delta y) \right\} \right. \\ &\quad \left. \times \left\{ \sum_m \Psi_{km} \beta_{km} \exp(-\beta_{km}(d_\mathrm{l} - d_\mathrm{s})) \cos\left(\alpha_m \left(\Delta z - \frac{c_\mathrm{l}}{2} \right) \right) \cosh(\beta_{km} \Delta y) \right\} \right] \end{aligned} \tag{13}$$

where the superscript * stands for the quantity's complex conjugate, and $y_1 = \Delta y$.

2.3. Guidance and levitation forces via LSM armature

The magnetic co-energy stored between the LSM armature coils on the ground and the onboard SCMs is

$$W'_m = \begin{pmatrix} i_U \\ i_V \\ i_W \end{pmatrix}^\mathrm{T} \begin{pmatrix} \psi_U \\ \psi_V \\ \psi_W \end{pmatrix} = \begin{pmatrix} i_d \\ i_q \\ i_0 \end{pmatrix}^\mathrm{T} \begin{pmatrix} \psi_d \\ \psi_q \\ \psi_0 \end{pmatrix} \tag{14}$$

where i_U, i_V, i_W and Ψ_U, Ψ_V, Ψ_W are the three-phase armature currents and flux linkages, respectively, while i_d, i_q, i_0 and Ψ_d, Ψ_q, Ψ_0 are those counterparts in $dq0$-axis. The guidance force that can be generated by the LSM armature is expressed in terms of $dq0$-axis variables:

$$\begin{aligned} F_\mathrm{Gpu} &= \frac{\partial W'_m(i_d, i_q, i_0, y_1)}{\partial y_1} = i_d \frac{\mathrm{d}\psi_d}{\mathrm{d}y_1} + i_q \frac{\mathrm{d}\psi_q}{\mathrm{d}y_1} + i_0 \frac{\mathrm{d}\psi_0}{\mathrm{d}y_1} \\ &= \sqrt{\frac{2}{3}} \sum_{k=1}^{\infty} \sum_{m=1}^{\infty} \beta_{km} \Psi_{km} \, \mathrm{e}^{\beta_{km} y_1} \{ k_d(x_1) i_d + k_q(x_1) i_q + k_0(x_1) i_0 \} \cong K_\mathrm{Gp}(y_1, t) i_d \end{aligned} \tag{15}$$

which represents the force for one unit feeding section of the LSM armature windings, where

$$\Psi_{km} = 2 n_\mathrm{a} \mu_0 \frac{\beta_{km}}{\alpha_k \alpha_m} \sin\left(\alpha_k \frac{l_\mathrm{a}}{2} \right) \sin\left(\alpha_m \frac{w_\mathrm{a}}{2} \right) a_\mathrm{s}(k, m) \mathrm{e}^{-\beta_{km}(d_\mathrm{a} - d_\mathrm{s})} \frac{\sin(N_\mathrm{a} \alpha_k \tau)}{\sin(2\alpha_k \tau)} \cos(\alpha_m z_1)$$

$$k_d(x_1) = k_{n_\mathrm{i}} \mathrm{e}^{\beta_{km} c_\mathrm{a}/2} (c_1 s_{u1} + c_2 s_{v1} + c_3 s_{w1}) + k_{n_\mathrm{o}} \mathrm{e}^{-\beta_{km} c_\mathrm{a}/2} (c_1 s_{u2} + c_2 s_{v2} + c_3 s_{w2})$$

$$k_q(x_1) = -k_{n_\mathrm{i}} \mathrm{e}^{\beta_{km} c_\mathrm{a}/2} (s_1 s_{u1} + s_2 s_{v1} + s_3 s_{w1}) - k_{n_\mathrm{o}} \mathrm{e}^{-\beta_{km} c_\mathrm{a}/2} (s_1 s_{u2} + s_2 s_{v2} + s_3 s_{w2})$$

$$k_0(x_1) = \frac{k_{n_i}\,\mathrm{e}^{\beta_{km}c_a/2}(s_{u1}+s_{v1}+s_{w1})}{\sqrt{2}} + \frac{k_{n_o}\,\mathrm{e}^{-\beta_{km}c_a/2}(s_{u2}+s_{v2}+s_{w2})}{\sqrt{2}}$$

$k_{n_i} = n_{ai}/n_a$, $k_{n_o} = n_{ao}/n_a$, n_{ai}, n_{ao}, n_a: number of turn for inner coil and outer coil, and the average number of turn for the armature:

$$c_1 = \cos\theta_{dq}, \qquad c_2 = \cos\left(\theta_{dq} - \frac{2\pi}{3}\right), \qquad c_3 = \cos\left(\theta_{dq} + \frac{2\pi}{3}\right), \qquad \theta_{dq} = \frac{\pi x_1}{\tau}$$

$$s_{u1} = \sin\left\{\alpha_k\left(x_1 + \frac{3\tau}{2}\right)\right\}, \qquad s_{u2} = \sin\left\{\alpha_k\left(x_1 - \frac{\tau}{2}\right)\right\}, \qquad s_{v1} = \sin\left\{\alpha_k\left(x_1 - \frac{7\tau}{6}\right)\right\}$$

$$s_{v2} = \sin\left\{\alpha_k\left(x_1 + \frac{5\tau}{6}\right)\right\}, \quad s_{w1} = \sin\left\{\alpha_k\left(x_1 + \frac{\tau}{6}\right)\right\}, \quad s_{w2} = \sin\left\{\alpha_k\left(x_1 - \frac{11\tau}{6}\right)\right\}$$

$$s_1 = \sin\theta_{dq}, \qquad s_2 = \sin\left(\theta_{dq} - \frac{2\pi}{3}\right), \qquad s_3 = \sin\left(\theta_{dq} + \frac{2\pi}{3}\right)$$

$$K_{Gp}(y_1, t) = \sqrt{\frac{2}{3}} \sum_{k=1,3,\cdots}^{\infty} \sum_{m=1,3,\cdots}^{\infty} \beta_{km}\Psi_{km}\,\mathrm{e}^{\beta_{km}y_1} k_d(x_1) \tag{16}$$

The coefficient K_{Gp} is the *guidance force coefficient of propulsion system* [4].

The vertical force utilized for levitation assist is expressed as

$$F_{vpu} = \frac{\partial W'_m(i_d, i_q, i_0, z_1)}{\partial z_1} \cong K_{vp}(z_1, t) i_d \tag{17}$$

where I_a, w_a, n_a: length, width and number of turn of the armature coil, N_a: number of cells for the unit feeding section. We have defined K_{vp} as the *vertical force coefficient of propulsion system* [5] given by the equation:

$$K_{vp} = \sqrt{\frac{2}{3}} \sum_{k=1}^{\infty} \sum_{m=1}^{\infty} \alpha_m \Psi_{km}\,\mathrm{e}^{\beta_{km}y_1} k_d(x_1) \tag{18}$$

3. Assist force control system design for lift and guidance

The dynamic governing equation of the maglev vehicle is then expressed as

$$M\frac{\mathrm{d}^2 y_1}{\mathrm{d}t^2} + F_{Gg}(t) = F_{Gpu}(t) \tag{19}$$

$$-F_{L_l}(t) + Mg - F_{vpu}(t) = M\frac{\mathrm{d}^2 \Delta z}{\mathrm{d}t^2} \tag{20}$$

We designed the lift controller as an LQI system, while designing the guidance controller as an LQ system. The two control systems were treated as separate SISO control systems based on the assumption that the magnetic spring for rolling motion [1] has sufficient magnitude to suppress the rolling motions at the speed of interest, although the dynamics has three axes of freedom: levitation, guidance and rolling. Fig. 3 shows our lift and guidance control system using the armature coil currents. The variable M is the vehicle mass. The levitation force and guidance force generated at the levitation–guidance coils were linearized when designing controllers:

$$F_{Gg}(t) \cong K_{yy}\Delta y(t) \tag{21}$$

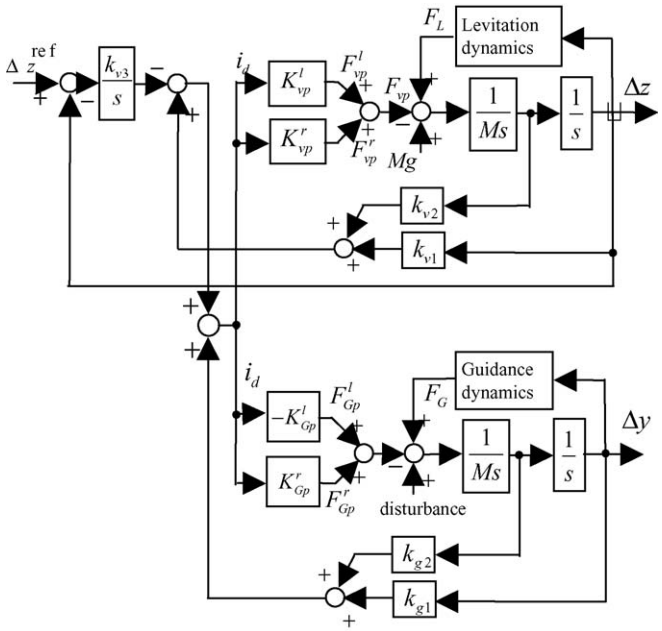

Fig. 3. Block diagram of lift and guidance assist system.

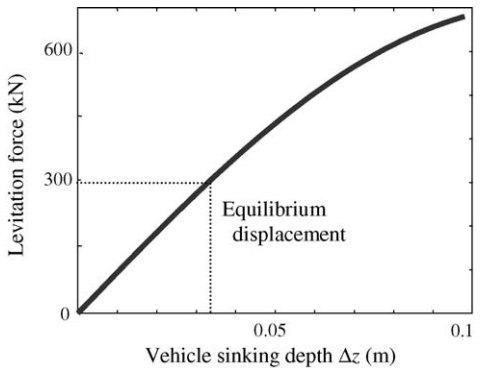

(a) Levitation force vs. vertical vehicle displacement (vehicle speed = 80km/h)

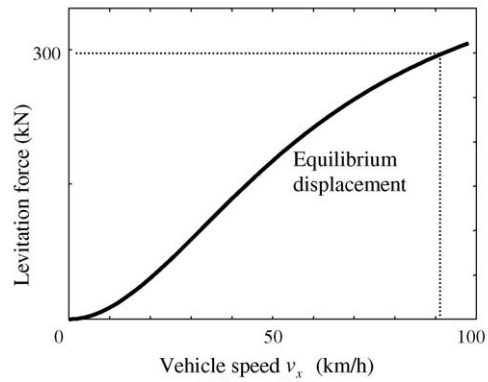

(b) Δz = 0.03m

Fig. 4. Levitation force characteristics of levitation–guidance coils.

Table 1
Dimensions of model

Vehicle mass	$M = 30000\,\text{kg}$
SCM	
Number of pole	8
Mmf	$n_s I_s = 700\,\text{kA}$
Pole pitch	$\tau = 2.1\,\text{m}$
Length, width	$l_s = 1.59\,\text{m}$, $w_s = 0.5\,\text{m}$
Levitation–guidance coil	
Length, width	$l_l = 0.55\,\text{m}$, $w_l = 0.31\,\text{m}$
LSM armature	
Length, width	$l_a = 2.1\,\text{m}$, $w_a = 0.7\,\text{m}$

$$F_{L_1}(t) \cong K_z \Delta z(t) + f_{L0} \tag{22}$$

where K_{yy}, K_z: the guidance spring modulus and the levitation spring modulus of the levitation–guidance coils, respectively, f_{L0}: constant.

4. Calculated results

4.1. Characteristics of model

Fig. 4(a) shows the levitation forces expressed in the unit of kN at the speed of 80 km/h generated by the levitation–guidance coils, being plotted as a function of the vehicle sinking depth Δz, which is the center height difference between the levitation coil and the SCM. When the sinking depth is 0, levitation force is surely not produced. The equilibrium point in the figure indicates the levitation force corresponding to the vehicle mass (30 ton → 294 kN of force). It is shown that the necessary force is generated with larger than the depth of about 0.033 m (3.3 cm) (Table 1).

The speed characteristics of the levitation force in the case of 0.03 m is shown in Fig. 4(b). The running velocity of over 90 km/h is needed to levitate the vehicle.

Fig. 5 shows the time average value of guidance force produced from the levitation–guidance coils as a function of the lateral displacement of vehicle.

The assist force coefficients of the propulsion system, i.e., LSM armature coils, are shown in Fig. 6: the vertical force coefficient is shown in Fig. 6(a), and the guidance force coefficient in Fig. 6(b).

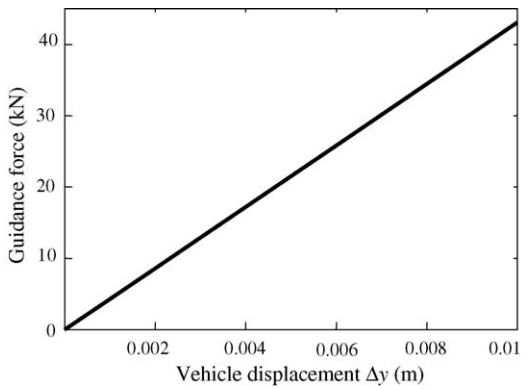

Fig. 5. Guidance force characteristics of Levitation–guidance coils (80 km/h).

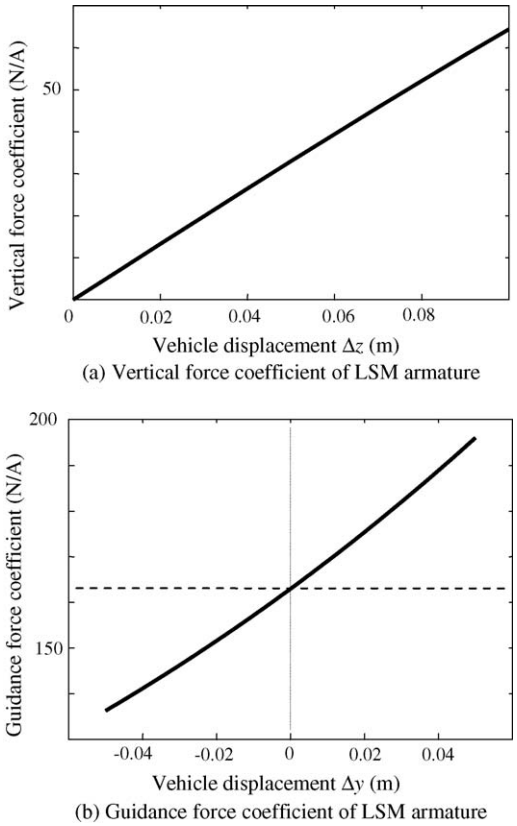

Fig. 6. Electromagnetic force coefficient of propulsion system.

4.2. Control system behaviors

The feedback gain vector for the lift control systems is given as

$$(k_{v1} \quad k_{v2} \quad k_{v3}) = (2.18 \times 10^4 \quad 2.00 \times 10^4 \quad 1.88 \times 10^4) \tag{23}$$

while the feedback gain vector for the guidance control systems is

$$(k_{g1} \quad k_{g2}) = (8.59 \times 10^3 \quad 5.62 \times 10^3) \tag{24}$$

Fig. 7 shows the computer simulation of the assist control system for lift and guidance forces at the speed of 80 km/h. The disturbance force of 10 kN was assumed in the simulation, which is the lateral wind flowing from the right side to the left side of the vehicle.

Since the reference of the vehicle sinking depth Δz is given to the control system, the d-axis LSM armature current has some magnitude to produce the assist levitation force (see Fig. 7b) at the initial state. This is because the levitation force generated from the levitation–guidance coils is not large enough to suspend the vehicle at the reference sinking depth of 0.03 m. At the instant the disturbance force is applied to the vehicle, the vehicle starts lateral movement to derail. Then the displacement (see Fig. 7f) causes not only the guidance force of levitation–guidance coils (see Fig. 7h), but also activates the assist guidance system to produce additional guidance forces (see Fig. 7c). The lateral displacement is controlled within about 1.5 mm by the control system (see Fig. 7f), while the vertical displacement, i.e., the vehicle sinking depth, is controlled very well (see Fig. 7e). The assist levitation and the levitation–guidance coil forces are about 26 and 268 kN on the average, respectively; the assist system produces 10% of the vehicle mass with the d-axis current of about 650 A. With respect to the guidance force, the assist system generates 9 kN, while the levitation–guidance coils 5.6 kN at most; the assist system produces about 60% of the total guidance force not to derail with the d-axis current of the maximum value of only about 30 A.

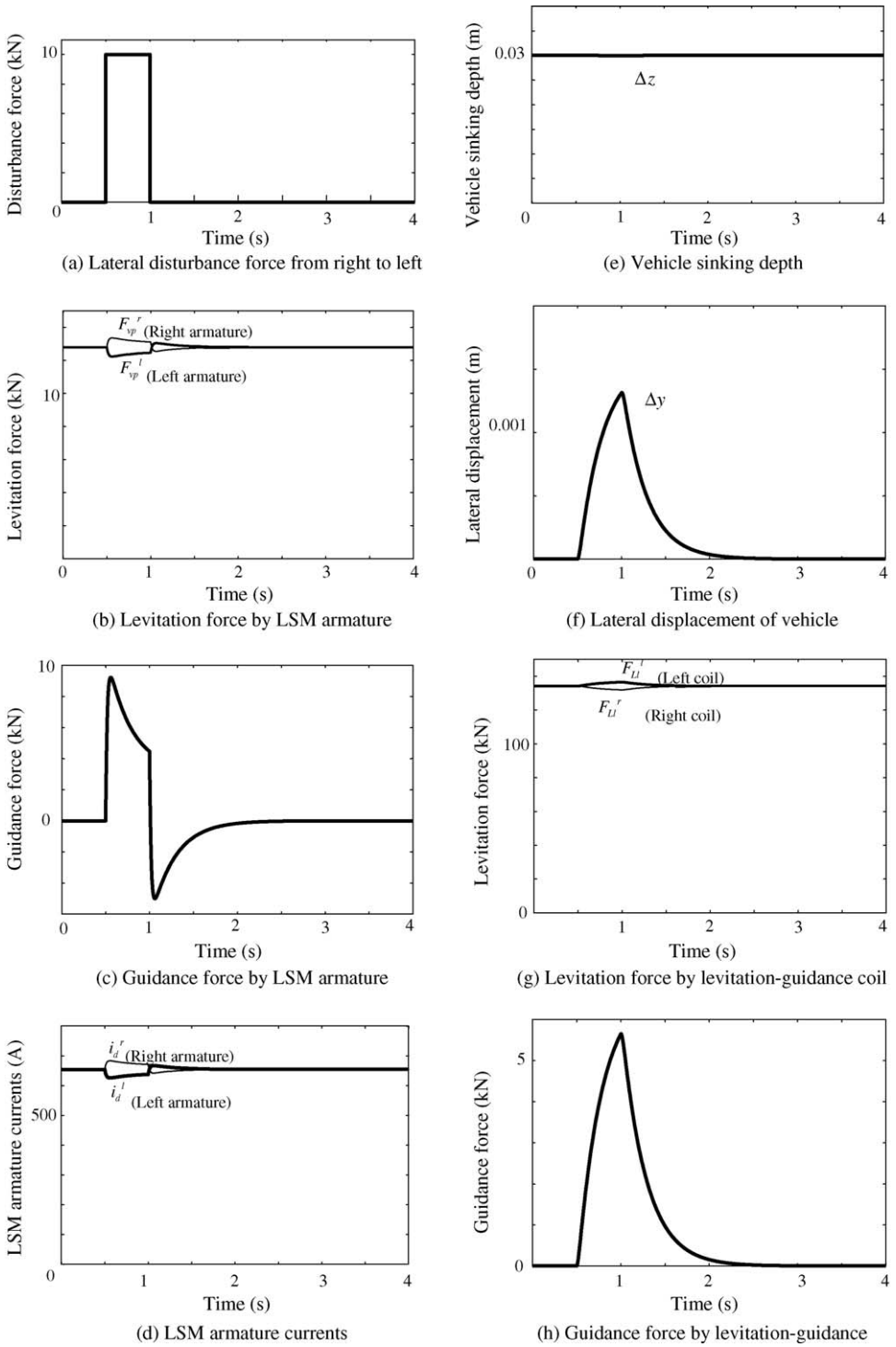

Fig. 7. Assist control system simulation (80 km/h).

5. Conclusion

We have presented the modelling and simulation of a superconducting maglev with an assist levitation and guidance mechanism employing the LSM armature currents. The electromagnetic forces of levitation–guidance coils and the LSM armature coils were shown as a function of speed and the displacements in order to design the assist control system. It was shown that the assist control system establishes a reference levitation height and the guidance performance. While the assist levitation needs large value of armature currents, guidance does not require much currents of LSM armature for the assist system to work.

References

[1] S. Fujiwara, Characteristics of EDS magnetic levitation having ground coils for levitation arranged on the side wall (in Japanese), IEEJ Trans. IA 108 (5) (1988) 439–446.
[2] T. Sakamoto, Mathematical treatment of superconducting linear synchronous motor, in: Proceedings of the Fourth International Symposium on Magnetic Suspension Technology, NASA/CP-1998-207654, 1998, pp. 211–220.
[3] T. Sakamoto, Investigation of superconducting linear synchronous motor propulsion control via an exact mathematical model, Electr. Eng. Jpn. 128 (2) (1999) 45–52.
[4] T. Sakamoto, Lateral force control through armature currents in superconducting LSM maglev vehicle, in: Proceedings of the Fifth International Symposium on Magnetic Suspension Technology, NASA/CP-2000-210291, 1999, pp. 51–61.
[5] T. Sakamoto, T. Kobayashi, Levitation force assist through LSM armature currents in superconducting maglev vehicle (in Japanese), IEEJ Trans. IA 124 (12) (2004) 1261–1267.
[6] T. Sakamoto, T. Shiromizu, Propulsion control of superconducting linear synchronous motor vehicle, IEEE Trans. Magn. 33 (5) (1997) 3460–3462.